

# The Observation of Percolation-Induced 2D Metal-Insulator Transition in a Si MOSFET

L. A. Tracy,<sup>1</sup> E. H. Hwang,<sup>2</sup> K. Eng,<sup>1</sup> G. A. Ten Eyck,<sup>1</sup> E. P. Nordberg,<sup>1</sup> K. C. Childs,<sup>1</sup> M. S. Carroll,<sup>1</sup> M. P. Lilly,<sup>1</sup> and S. Das Sarma<sup>2</sup>

<sup>1</sup>Sandia National Laboratories, Albuquerque, NM 87185

<sup>2</sup>Condensed Matter Theory Center, Department of Physics,  
University of Maryland, College Park, MD 20742-4111

(Dated: February 21, 2024)

By analyzing the temperature ( $T$ ) and density ( $n$ ) dependence of the measured conductivity ( $\sigma$ ) of 2D electrons in the low density ( $\sim 10^{11} \text{ cm}^{-2}$ ) and temperature (0.02 – 10 K) regime of high-mobility ( $1.0$  and  $1.5 \times 10^4 \text{ cm}^2/\text{Vs}$ ) Si MOSFETs, we establish that the putative 2D metal-insulator transition is a density-inhomogeneity driven percolation transition where the density-dependent conductivity vanishes as  $(n - n_p)^p$ , with the exponent  $p \approx 1.2$  being consistent with a percolation transition. The ‘metallic’ behavior of  $\sigma(T)$  for  $n > n_p$  is shown to be well-described by a semi-classical Boltzmann theory, and we observe the standard weak localization-induced negative magnetoresistance behavior, as expected in a normal Fermi liquid, in the metallic phase.

The so-called two-dimensional (2D) metal-insulator transition (MIT) has been a subject<sup>1,2</sup> of intense activity and considerable controversy ever since the pioneering experimental discovery<sup>3</sup> of the 2D MIT phenomenon in Si MOSFETs by Kravchenko and Pudalov some fifteen years ago. The apparent MIT has now been observed in almost all existing 2D semiconductor structures, including Si MOSFETs<sup>3,4</sup>, electrons<sup>5,6,7</sup> and holes<sup>8,9,10,11</sup> in GaAs/AlGaAs, and electrons in Si/SiGe<sup>12,13</sup> systems. The basic phenomenon refers to the observation of a carrier density-induced qualitative change in the temperature dependence of the resistivity ( $\rho(T)$ ), where  $n_c$  is a critical density separating an ‘active metallic’ phase ( $n > n_c$ ) from an ‘insulating’ phase ( $n < n_c$ ), exhibiting  $d\rho/dT > 0$  ( $< 0$ ) behavior typical of a metal (insulator).

The high-density metallic behavior ( $n > n_c$ ) often manifests in a large (by 25% for electrons in GaAs/AlGaAs heterostructures to factors of 2–3 in Si MOSFETs) increase in resistivity with increasing temperature in the low temperature (0.05 – 5 K) regime where phonons should not play much of a role in resistive scattering. The insulating regime, at least for very low ( $n < n_c$ ) densities and temperatures, seems to be the conventional activated transport regime of a strongly localized system. The 2D MIT phenomenon occurs in relatively high-mobility systems although the mobility values range from  $10^4 \text{ cm}^2/\text{Vs}$  (Si MOSFET) to  $10^7 \text{ cm}^2/\text{Vs}$  (GaAs/AlGaAs) depending on the 2D system under consideration. The 2D MIT phenomenon is also considered to be a low-density phenomenon although, depending on the 2D system under consideration, the critical density  $n_c$  differs by two orders of magnitude ( $n_c \sim 10^{11} \text{ cm}^{-2}$  in 2D Si and  $10^9 \text{ cm}^{-2}$  in the high-mobility GaAs/AlGaAs heterostructures). The universal features of the 2D MIT phenomenon are: (1) the existence of a critical density  $n_c$  distinguishing an ‘active high-density metallic’ ( $d\rho/dT > 0$  for  $n > n_c$ ) phase from an ‘active low-density insulating’ ( $d\rho/dT < 0$  for  $n < n_c$ ) phase; and (2) while the insulating phase for  $n < n_c$  seems mostly to

manifest the conventional activated transport behavior, the metallic temperature dependence at low ( $n \approx n_c$ ) densities is universal in the sense that it manifests a very strong temperature dependence, not seen in standard 3D metals where  $\rho(T)$  is temperature independent in the  $T < 10 \text{ K}$  Bloch-Grüneisen transport regime.

The excitement and controversy in the subject arise from the deep conceptual questions associated with the nature of the MIT and the metallic phase. In particular, it is theoretically well-established<sup>1</sup> that a non-interacting (or weakly interacting) disordered 2D electron system is an insulator at  $T = 0$ , and therefore it follows<sup>1</sup> that if the 2D MIT is a true  $T = 0$  quantum phase transition (QPT), then the 2D metallic phase, if it survives all the way to  $T = 0$ , must necessarily be a novel and exotic non-Fermi liquid phase since it cannot be connected adiabatically to the non-interacting 2D electron system, which is always localized in the presence of any disorder. The alternative possibility<sup>2</sup> is that the metallic phase is allowed only at finite temperatures, and the 2D MIT is not a QPT, but a density-induced crossover from a weakly localized ‘active’ metallic phase to a strongly localized insulator. These two qualitatively distinct viewpoints have both received support in the literature, and experimental results have been presented claiming support for the QPT<sup>14</sup> and the finite-temperature crossover<sup>7,11</sup> viewpoints, respectively. Whether the observed 2D MIT is a novel ( $T = 0$ ) QPT leading to an exotic 2D non-Fermi liquid metallic phase established by interaction effects or is a finite-temperature crossover between an ‘active’ metallic phase and the insulating phase is obviously a question of great fundamental importance.

Previous measurements of 2D MIT phenomena in Si MOSFETs have been discussed in terms of quantum critical phenomena<sup>1,14</sup>. However, for 2D electrons and holes in high mobility GaAs/AlGaAs heterostructures, it has been shown that the 2D MIT can be described as a percolation transition<sup>7,11,15</sup>. Thus, a natural question to ask is whether the 2D MIT in Si MOSFETs is really different

than for GaAs systems, or whether both Si and GaAs 2D systems undergo the same universal percolation-driven transition. The Si MOSFET is different than GaAs systems in that it has much lower mobility and the disorder in Si MOSFETs is thought to be dominated by 'short-range' scattering, which is potentially different than for other 2D systems, such as in GaAs where 'long-range' scattering may play a larger role. This point has been recently emphasized in the literature and it has been proposed that the physics behind the 2D MIT for Si MOSFETs versus GaAs systems may differ due to differences in mobility and range of the disorder potential (short vs. long-range scattering)<sup>14</sup>.

In this article, we provide the first experimental evidence that the MIT for Si MOSFETs is a finite-temperature, density inhomogeneity driven semi-classical percolation transition, and is therefore not a QPT. Our work shows that the 2D MIT is a universal percolation transition for both GaAs and Si, in contrast to claims of a QPT in Si<sup>14</sup>. As mentioned earlier, the 2D MIT in high-mobility GaAs electron and hole systems has already been experimentally demonstrated to be a percolation transition<sup>7,11,15</sup>, but our work provides the first compelling evidence supporting the percolation scenario in Si MOSFETs. We also establish that the metallic phase is a conventional Fermi liquid by showing that (1) the measured transport properties in the effective metallic phase qualitatively agree very well with the conclusions of a semi-classical Boltzmann transport theory<sup>16</sup> taking into account the detailed density and temperature dependence of carrier screening properties, and (2) the expected negative magnetoresistance signature of the conventional weak localization behavior<sup>17</sup> is clearly manifest experimentally in the effective metallic phase of our samples.

The two samples used in this study are Si MOSFET structures with a peak mobility of  $1.5 \times 10^4 \text{ cm}^2/\text{Vs}$  (sample A) and  $1 \times 10^4 \text{ cm}^2/\text{Vs}$  (sample B). For both samples, the 2D electron gas (2DEG) resides at the Si-SiO<sub>2</sub> gate oxide interface, where the SiO<sub>2</sub> thickness is nominally 35 nm for sample A and 10 nm for sample B. The gate oxide is thermally grown in dry O<sub>2</sub> at 900 °C on FZ (100)-oriented high-resistivity ( $> 5 \text{ k}\Omega\text{-cm}$  for sample A and  $> 100 \text{ }\Omega\text{-cm}$  for sample B, at room temperature) p-type Si wafers. Ohmic contacts to the 2DEG consist of n<sup>+</sup> Si regions formed by implantation of As; these contacts are not self-aligned, but are instead patterned and implanted before the gate oxide growth. An n<sup>+</sup> polySi gate, patterned to form a 15  $\mu\text{m}$   $\times$  100  $\mu\text{m}$  Hallbar, is used to induce carriers. The 2DEG resistivity is experimentally determined via standard four-terminal lock-in measurements and the density is calibrated via measurements of the Hall resistivity.

In Fig. 1 we show the density-dependent mobility of samples A and B along with the theoretically calculated mobility curves. Our theoretical calculations<sup>18</sup> include the temperature-dependent nitewavevector screening of the charged impurity Coulomb scattering and the short-

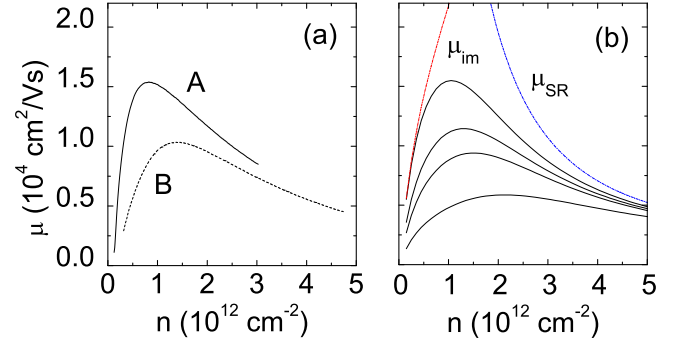


FIG. 1: (color online) (a) Experimental mobility  $\mu$  as a function of density  $n$  for two samples, A and B, at a temperature  $T = 0.25 \text{ K}$ . (b) Theoretical mobility as a function of density. High (low) density mobility is limited by the surface roughness ( $\mu_{\text{SR}}$  (charged impurity  $\mu_{\text{im}}$ ) scattering. Different curves correspond to different charged impurity densities ( $n_i = 6; 9; 12$ , and  $24 \times 10^{10} \text{ cm}^{-2}$  from top to bottom), but with the same surface roughness ( $\alpha = 1.9 \text{ \AA}$ ,  $\alpha = 26 \text{ \AA}$ ).

range surface roughness scattering at the Si-SiO<sub>2</sub> interface. It is well-known that the long-range charged impurity scattering and the short-range surface roughness scattering dominate respectively the low and the high carrier density regimes of transport in Si MOSFETs<sup>19</sup>. We show Fig. 1a and b together to allow the reader to judge the level of agreement between experiment and theory, which depends on several scattering parameters (e.g. the density and spatial distribution of charged impurity centers in the sample and the height and lateral correlation functions of the interface roughness function). The mobility ( $\mu$ ) first rises steeply with density ( $n$ ) reaching a maximum at a characteristic density  $n_m$ , beyond which it falls off slowly with increasing  $n$ , due to short-range surface roughness scattering at the Si-SiO<sub>2</sub> interface<sup>19</sup>. At low carrier densities ( $n < 10^{12} \text{ cm}^{-2}$ ) however, long-range Coulomb scattering by unintentional random charged impurities invariably present on the insulating oxide side of the Si-SiO<sub>2</sub> interface dominates the 2D mobility, and, as has been emphasized<sup>20</sup> in the literature, all Si 2D MIT behavior manifests itself at low carrier densities ( $n \sim 10^{11} \text{ cm}^{-2}$ ) where the charged impurity scattering dominates transport and the short-range interface roughness scattering is negligible. We emphasize the fact that the 2D MIT phenomenon (i.e.  $n_c$  and the density range for the 'anomalous' metallic phase with a strongly temperature dependent 2D resistivity) occurs in the density regime  $n \sim 10^{11} \text{ cm}^{-2}$  which, being substantially below  $n_m$ , is completely dominated by the long-range screened Coulomb scattering. This dominance of Coulomb scattering in the 2D MIT physics is crucial for the percolation physics which arises from the nonlinear failure of screening of the long-range Coulombic charged impurity potential, to be discussed below. The short-range surface-roughness scattering, which dominates MOSFET transport for  $n > 10^{12} \text{ cm}^{-2}$ , plays no role in the 2D MIT phenomena since both the

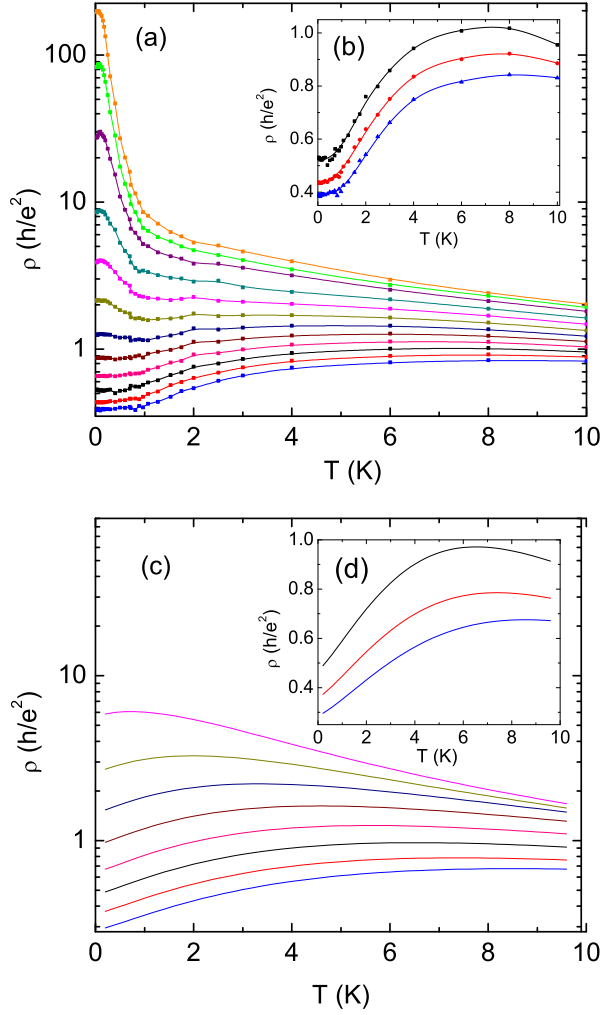


FIG. 2: (color online) (a) Experimental resistivity in units of  $h/e^2$  as a function of temperature for sample A at 2D electron densities (from top to bottom)  $n = 1.07; 1.10; 1.13; 1.20; 1.26; 1.32; 1.38; 1.44; 1.50; 1.56; 1.62$ , and  $1.68 \times 10^{11} \text{ cm}^{-2}$ . Inset (b) Enlarged view of data in the effective metallic regime at  $n = 1.56; 1.62$ , and  $1.68 \times 10^{11} \text{ cm}^{-2}$ . Solid lines are guides to the eye. (Data below 0.1 K may not be reliable due to electron heating.) (c) Theoretically calculated temperature and density dependent resistivity for sample A for densities  $n = 1.26; 1.32; 1.38; 1.44; 1.50; 1.56; 1.62$ , and  $1.68 \times 10^{11} \text{ cm}^{-2}$  (from top to bottom). Inset shows the resistivities for  $n = 1.56; 1.62$ , and  $1.68 \times 10^{11} \text{ cm}^{-2}$ .

critical density for the transition and the density regime where the strong metallic behavior (i.e. the strong temperature dependence of the 2D conductivity) is observed are well below the operational regime of the short-range surface roughness scattering.

In Fig. 2 we show our measured (Fig. 2(a) – (b)) and calculated (Fig. 2(c) – (d)) temperature and density dependent resistivity ( $\rho(T; n)$ ) for sample A with the maximum mobility of  $1.5 \times 10^4 \text{ cm}^2/\text{Vs}$  (see Fig. 1(a)). The results for sample B are similar, but with a larger value of the critical density,  $n_c \approx 2.5 \times 10^{11} \text{ cm}^{-2}$  (and

somewhat weaker temperature dependence), consistent with its lower (and consequently, higher disorder) peak mobility  $1 \times 10^4 \text{ cm}^2/\text{Vs}$ . The classic 2D MIT behavior is apparent in Fig. 2(a) where  $\rho(T)$  for various densities manifests the clear distinction between metallic ( $d\rho/dT > 0$ ) and insulating ( $d\rho/dT < 0$ ) behavior separated (visually) by a critical density  $n_c \approx 1.4 \times 10^{11} \text{ cm}^{-2}$ . We note that the temperatures quoted in Fig. 2a and b are those of the cryostat cold finger; although the resistivity continues to evolve below  $T \approx 100 \text{ mK}$  (albeit slowly), we cannot claim in this regime ( $T < 100 \text{ mK}$ ) that the 2D electrons and the cold finger are in thermal equilibrium down to the base temperature of our cryostat (20 mK). The inset in Fig. 2(b) shows in detail the metallic behavior for  $n > n_c$ , which manifests more than a factor of 2 increase in  $\rho(T)$  for  $T \approx 0.1 - 7 \text{ K}$  before decreasing slightly at higher temperatures. The strong initial increase in  $\rho(T)$  with  $T$  arises<sup>16</sup> from the temperature-induced weakening of screening at these low densities as  $T=T_F$  increases from 0.01 at low temperatures essentially to 1 at  $T \approx 8 \text{ K}$  since  $T_F \approx 7.3 \text{ K}$  for  $n = 10^{11} \text{ cm}^{-2}$ . (Phonon scattering is unimportant in Si MOSFET for  $T < 10 \text{ K}$ .)

Finally, in Fig. 2(c) we show our theoretically calculated  $\rho(T; n)$  where the Boltzmann transport is calculated using the screened charged impurity scattering as the only resistive scattering mechanism<sup>16</sup>. Although the ratio of the Coulomb to Fermi energy,  $r_s$ , can be as large as  $\approx 15$  near the MIT for this sample, suggesting that Coulomb interactions could play an important role, we note that the basic features of the experimental metallic phase are well-captured by the screening theory with  $\rho(T)$  rising approximately by a factor of 2 initially and then decreasing slightly at higher (lower) temperatures (densities) around  $T=T_F$  & 1 due to quantum-classical crossover<sup>16</sup>. The theoretical results, following the work of Ref.<sup>16</sup>, are being shown here in order to demonstrate that a realistic semiclassical transport theory including the screened long-range scattering by charged impurities completely captures all the main features of the experimental results with the basic physics being a strong temperature and density dependent modification in the effective screened disorder due to the large change in the effective  $T=T_F$  in the experimental  $T \approx 0.1 - 10 \text{ K}$  temperature range. We point out that, by definition, the theoretical transport results in Figs. 2(c) and (d) apply only in the metallic regime since the metal-insulator transition cannot be captured in a Boltzmann theory.

Having established the phenomenology of the 2D MIT behavior in Fig. 2, we now come to the nature of the density driven transition itself. We plot in Fig. 3 our measured conductivity ( $\sigma$ ) as a function of  $n$  to see if a percolation behavior,  $\sigma(n) \propto (n - n_p)^p$ , where  $n_p, p$  are the percolation transition density and exponent respectively, is manifested. Our fits yields  $p \approx 1.20$ ,  $n_p \approx 1.2 \times 10^{11} \text{ cm}^{-2}$  for sample A and  $p \approx 1.24$ ,  $n_p \approx 2.0 \times 10^{11} \text{ cm}^{-2}$  for sample B. The fits describe  $\sigma(n)$  well over nearly two orders of magnitude change in conductivity. The devia-

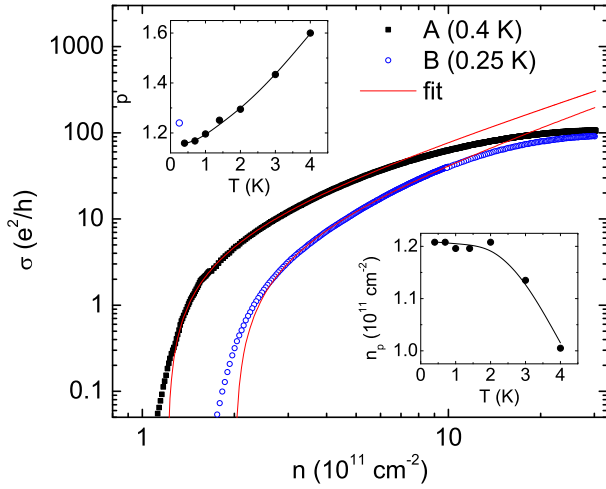


FIG. 3: (color online) (a) Main plot: Points show experimental conductivity in units of  $e^2/h$  versus electron density  $n$  for sample A at  $T = 0.4$  K (closed symbols) and B at  $T = 0.25$  K (open symbols). The solid lines are fits to the data of the form  $\sigma = A(n - n_p)^p$ . The upper and lower insets show the exponent  $p$  and critical density  $n_p$ , respectively, as a function of temperature for sample A. Solid lines are a guide to the eye. The open symbol in the upper inset shows  $p$  for sample B at  $T = 0.25$  K.

tions of the fit from the data seen at the lowest densities ( $n < n_c$ ) are expected since our percolation analysis applies only in the metallic regime. At high densities the fit is also expected to deviate since the percolation fit is a critical scaling behavior which is expected to be best for densities close to  $n_p$ , and also the role of surface roughness scattering becomes increasingly important at high densities. The fact that our best fit values of  $n_p$  and  $p$  for sample A are almost independent of temperature at low temperatures is a good indicator for the percolation transition being the correct description for the 2D MIT phenomenon shown in Fig. 2. Our numerically extracted best-fit exponent  $p = 1.2$  is sufficiently close to the percolation conductivity exponent of 1.31 for us to feel confident that the observed 2D MIT in Si MOSFETs is a density inhomogeneity-driven percolation transition.

In Fig. 4, we show an alternate (and perhaps more appropriate, if the transition is indeed a percolation transition) method of extracting the critical density from a percolation fit, where we hold both the exponent  $p$  and the prefactor  $A$  fixed, and allow only  $n_p$  to vary. We use  $p = 1.31$ , the value expected for percolation in 2D, and determine  $A$  from the percolation fit to the  $T = 0.4$  K data, as shown in the inset to Fig. 4, also holding  $p = 1.31$  fixed. If the 2D MIT is indeed a percolation transition, then this method of obtaining  $n_p$  is more appropriate than allowing  $p$  to vary since the exponent is universal and the critical density is not. As seen in the inset to Fig. 4, the fit to our  $\sigma$  vs.  $n$  data with  $p = 1.31$  fixed is very good. As can be seen from the main figure, the extracted  $n_p$  obtained via this method decreases with

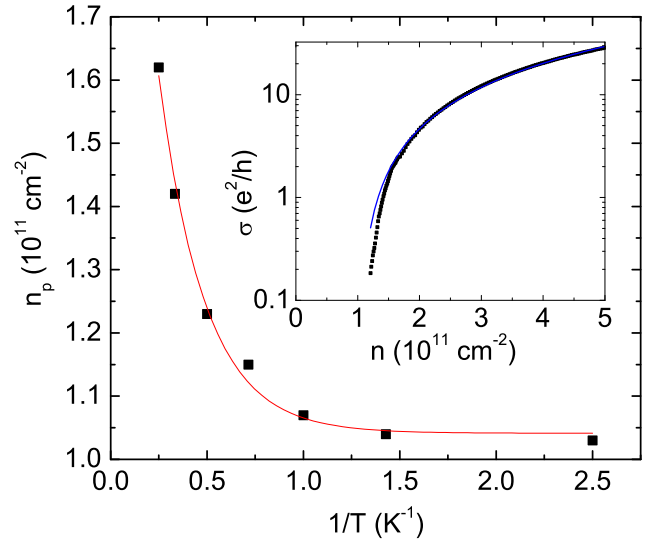


FIG. 4: (color online) Main plot: Points show  $n_p$  vs.  $1/T$  obtained from a percolation fit to the  $\sigma$  vs.  $n$  data performed by holding the exponent  $p = 1.31$  fixed (see text). The solid trace is a fit of the form  $n_p = n_0 + A e^{b/T}$ . Inset: Points show experimental data  $\sigma$  vs.  $n$  for sample A at  $T = 0.4$  K, while the solid line is a percolation fit with fixed  $p = 1.31$ .

decreasing temperature, eventually saturating at the lowest temperatures. A fit of the form  $n_p = n_0 + A e^{b/T}$  is shown as the solid line in the main plot of Fig. 4. The fit yields  $n_p = 1.04 + 1.62 e^{4.20/T}$ . The parameter  $b = 4.2$  K is an effective "energy gap" that can be calculated if the impurity distribution is known. We note that this implies a  $T = 0$  MIT transition density of  $1.04 \times 10^{11} \text{ cm}^{-2}$ , which is considerably less than the nominal critical density of  $1.4 \times 10^{11} \text{ cm}^{-2}$  one would have inferred from the temperature-dependent resistivity behavior in Fig. 2(a). The fact that the temperature-dependent resistivity by itself gives a strong over-estimate of the 2D MIT critical density is already known in the literature.

In Fig. 5 we show our observed weak localization behavior by plotting the expected<sup>17</sup> negative magnetoresistance in the metallic phase as a function of an applied weak magnetic field. The weak localization data in Fig. 5 is fitted to the standard digamma function behavior expected of a disordered 2D system<sup>17</sup>

$$\sigma = \frac{e^2}{h} g_v \left[ \frac{1}{2} + \frac{B}{2} \right]^{-1} = \frac{e^2}{h} g_v \left[ \frac{1}{2} + \frac{B}{2} \right]^{-1}; \quad (1)$$

where  $B = 4eB_z D$  and  $D$  is the diffusion coefficient. The behavior is quite normal, explicitly demonstrating that our observed metallic phase ( $n > n_c; n_p$ ) is indeed the usual weakly localized Fermi liquid metallic phase, and not some exotic non-Fermi liquid  $T = 0$  metal. The observation of the expected weak localization behavior in the 2D metallic phase along with the percolative nature of the transition is strong evidence that the experimental 2D MIT is not a QPT, but a crossover.

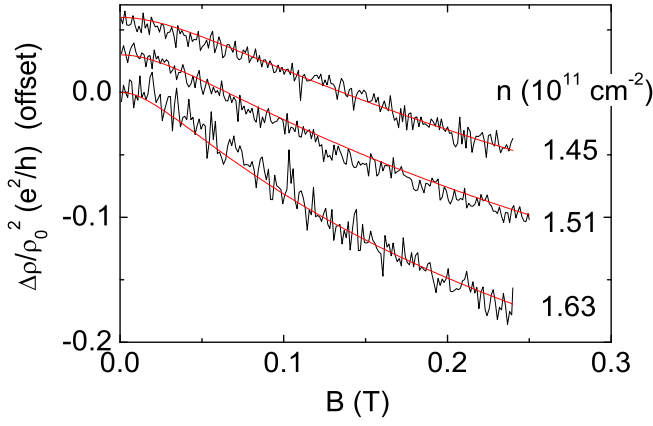


FIG. 5: (color online) Measured weak localization correction to the resistivity,  $\Delta\rho/\rho_0^2$  in units of  $e^2/h$  (with offset for clarity) versus perpendicular magnetic field  $B$  at densities  $n = 1.51, 1.45$ , and  $1.63 \times 10^{11} \text{ cm}^{-2}$  at  $T = 100 \text{ mK}$ . The red lines are fits to the standard weak localization correction (see text). The momentum relaxation times are determined from the mobility, while the weak localization fits yield a correction amplitude  $\gamma = 0.25$  and phase relaxation time  $\tau_\phi = 33, 32$ , and  $28 \text{ ps}$  (top to bottom).

Before concluding, we briefly discuss the physics underlying the percolation transition. As emphasized above, the 2D MIT phenomenon occurs in the transport regime dominated by long-range Coulombic charged impurity scattering. It was pointed out some years ago<sup>21</sup> that such a transport regime is susceptible at low carrier densities to a semiclassical percolation MIT since large scale density inhomogeneities (i.e. puddles) could appear in the system due to the nonlinear failure of screening of the charged impurities at low carrier densities. One can approximately estimate<sup>21</sup> the percolation transition density,  $n_p$ , by considering the inhomogeneous density fluctuations in the system, leading to  $n_p \approx 0.2 \bar{n}_i/d$ , where  $n_i$  is the effective 2D charged scatterer density and  $d$  is the effective separation between the 2D carriers and the scatterers. Using  $n_i = 6$  and  $11 \times 10^{10} \text{ cm}^{-2}$ , the value needed to get the correct mobility at higher densities for sample A and B, respectively (these values of  $n_i$  are roughly consistent with C-V measurements which estimate the density of fixed charge near the Si-SiO<sub>2</sub> interface to be  $8 \times 10^{10} \text{ cm}^{-2}$ ), and taking  $d \approx 5-6 \text{ nm}$ , which is consistent with the 2D electron layer in the Si MOSFET being about  $5 \text{ nm}$  away from the interface due to the self-consistent potential produced by the electrons themselves, we get  $n_p \approx 0.9$  and  $1.2 \times 10^{11} \text{ cm}^{-2}$  for sample A and B, respectively, which is close to our experimentally extracted percolation density in Fig. 3(a). (We note that  $d$  corresponds to the effective separation between the 2D electrons and the charged impurities,

which must incorporate the fact that the 2D electrons are on the average about  $5 \text{ nm}$  inside Si at  $n \approx 10^{11} \text{ cm}^{-2}$ .) The 2D conductivity percolation exponent is numerically known to be around  $1.31$ , which is close to the exponent value ( $1.20$  for sample A,  $1.24$  for sample B) we get in our analysis. Finally, we note that the puddles produced by the nonlinear failure of screening of charged impurities in low-density 2D systems have been directly observed in 2D GaAs<sup>22</sup> systems.

In conclusion, we have experimentally established that the 2D MIT in Si MOSFETs is a percolation-induced transition driven by the dominance of the long-range charged impurity disorder. At low carrier densities, the failure of linear screening leads to the formation of inhomogeneous puddles in the 2D density landscape, which then produces a semiclassical percolation transition. The nature of the percolation transition and the effective metallic phase is the same in Si MOSFETs and 2D GaAs electron<sup>7</sup> and hole<sup>11</sup> systems. The metallic temperature dependence arises from the strong temperature dependence of screening and the percolation transition arises from the low-density failure of screening. The 2D MIT is therefore a quantum crossover phenomenon, not a QPT, from an effective (weakly localized) metallic phase to a strongly localized insulating phase. The agreement between the percolative conductivity and our experimental work as well as our finding of the usual weak localization effect in our data conclusively rules out quantum criticality in the 2D MIT phenomena. Our work establishes that the 2D MIT is a universal percolation-driven transition, caused by the inhomogeneous density landscape induced by charged impurities at low carrier densities, in both GaAs-based systems<sup>7,11,15</sup> as well as in Si MOSFETs (our work). Screening of the charged impurity scattering produces the strong temperature dependence of the apparent metallic phase since low carrier densities automatically imply large values of  $T = T_F$ , and the eventual failure of screening at still lower densities, where there are just too few carriers to effectively screen the impurity charges, leads to the percolation MIT since the 2D system becomes inhomogeneous due to the formation of puddles.

#### Acknowledgments

This work was performed, in part, at the Center for Integrated Nanotechnologies, a U.S. DOE, Office of Basic Energy Sciences user facility. Sandia National Laboratories is a multi-program laboratory operated by Sandia Corporation, a Lockheed-Martin Company, for the U.S. Department of Energy under Contract No. DE-AC04-94AL85000.

<sup>1</sup> S. V. Kravchenko and M. P. Sarachik, Rep. Prog. Phys. 67, 1 (2004); E. Abraham, S. V. Kravchenko, and M. P.

Sarachik, Rev. Mod. Phys. 73, 251 (2001).

- <sup>2</sup> S.D as Samra and E.H.Hwang, Solid State Commun. 135, 579 (2005).
- <sup>3</sup> S.V.Kravchenko et al., Phys. Rev. B 50, 8039 (1994).
- <sup>4</sup> S.V.Kravchenko et al., Phys. Rev. B 51, 7038 (1995).
- <sup>5</sup> Y.Hanein et al., Phys. Rev. B 58, R13338 (1998).
- <sup>6</sup> M.P.Lilly et al., Phys. Rev. Lett. 90, 056806 (2003).
- <sup>7</sup> S.D as Samra et al., Phys. Rev. Lett. 94, 136401 (2005).
- <sup>8</sup> Y.Hanein et al., Phys. Rev. Lett. 80, 1288 (1998).
- <sup>9</sup> M.Y.Simmons et al., Phys. Rev. Lett. 80, 1292 (1998).
- <sup>10</sup> A.P.Mills et al., Phys. Rev. Lett. 83, 2805 (1999).
- <sup>11</sup> M.J.Manfra et al., Phys. Rev. Lett. 99, 236402 (2007).
- <sup>12</sup> K.Lai et al., Phys. Rev. B 72, 081313 (2005).
- <sup>13</sup> K.Lai et al., Phys. Rev. B 75, 033314 (2007).
- <sup>14</sup> S.Anissimova et al., Nat. Phys. 3, 707 (2007).
- <sup>15</sup> R.Letourcq et al., Phys. Rev. Lett. 90, 076402 (2003); Y.Meir, Phys. Rev. Lett. 83, 3506 (1999); G.Allison et al., Phys. Rev. Lett. 96, 216407 (2006); L.A.Tracy et al., Solid State Commun. 137, 150 (2006); Y.Hanein et al., Phys. Rev. B 58, R7520 (1998).
- <sup>16</sup> S.D as Samra and E.H.Hwang, Phys. Rev. Lett. 83, 164 (1999); Phys. Rev. B 68, 195315 (2003); Phys. Rev. B 69, 195305 (2004).
- <sup>17</sup> P.A.Lee and T.V.Ramakrishnan, Rev. Mod. Phys. 57, 287 (1985); S.Hikami, A.Larkin, and Y.Nagaoka, Prog. Theor. Phys. 63, 707 (1980).
- <sup>18</sup> All calculations are carried out following the prescription described in refs.16 above, where all the theoretical details are available.
- <sup>19</sup> T.Ando, A.B.Fowler, and F.Stem, Rev. Mod. Phys. 54, 438 (1982).
- <sup>20</sup> T.M.Klapwijk and S.D as Samra, Solid State Commun. 110, 581 (1999).
- <sup>21</sup> A.L.Efros, Solid State Commun. 65, 1281; 70, 253 (1989); S.He and X.C.Xie, Phys. Rev. Lett. 80, 3324 (1998); J.A.Nixon and J.Davies, Phys. Rev. B 41, 7929 (1990); A.L.Efros et al., Phys. Rev. B 47, 2233 (1993); J.Shi and X.C.Xie, Phys. Rev. Lett. 88, 086401 (2002).
- <sup>22</sup> S.Ilaniet al., Phys. Rev. Lett. 84, 3133 (2000).